Mathematical Biosciences and Engineering

http://www.aimspress.com/journal/MBE

MBE, 19(12): 13114–13136.
DOI: 10.3934/mbe.2022613
Received: 30 May 2022
Accepted: 28 August 2022
Revised: 23 August 2022
Published: 06 September 2022

Research article

Unravelling the dynamics of Lassa fever transmission with differential infectivity: Modeling analysis and control strategies

Salihu S. Musa[1,2,*], Abdullahi Yusuf[3], Emmanuel A. Bakare[4,5], Zainab U. Abdullahi[6], Lukman Adamu[7], Umar T. Mustapha[8] and Daihai He[1,*]

[1] Department of Applied Mathematics, Hong Kong Polytechnic University, Hong Kong, China
[2] Department of Mathematics, Kano University of Science and Technology, Wudil, Kano, Nigeria
[3] Department of Computer Engineering, Biruni University, Istanbul, Turkey
[4] Department of Mathematics, Federal University Oye Ekiti, Ekiti, Nigeria
[5] Biomathematics and Applied Mathematical Modelling Research Group, Federal University Oye Ekiti, Ekiti, Nigeria
[6] Department of Biological Sciences, Federal University Dutsin-Ma, Katsina, Nigeria
[7] Department of Mathematical Sciences, Faculty of Science, University of Maiduguri, Nigeria
[8] Department of Mathematics, Science Faculty, Federal University Dutse, Jigawa, Nigeria

* **Correspondence:** Email: salihu-sabiu.musa@connect.polyu.hk, daihai.he@polyu.edu.hk.

Abstract: Epidemic models have been broadly used to comprehend the dynamic behaviour of emerging and re-emerging infectious diseases, predict future trends, and assess intervention strategies. The symptomatic and asymptomatic features and environmental factors for Lassa fever (LF) transmission illustrate the need for sophisticated epidemic models to capture more vital dynamics and forecast trends of LF outbreaks within countries or sub-regions on various geographic scales. This study proposes a dynamic model to examine the transmission of LF infection, a deadly disease transmitted mainly by rodents through environment. We extend prior LF models by including an infectious stage to mild and severe as well as incorporating environmental contributions from infected humans and rodents. For model calibration and prediction, we show that the model fits well with the LF scenario in Nigeria and yields remarkable prediction results. Rigorous mathematical computation divulges that the model comprises two equilibria. That is disease-free equilibrium, which is locally-asymptotically stable (LAS) when the basic reproduction number, $\mathcal{R}_0$, is < 1; and endemic equilibrium, which is globally-asymptotically stable (GAS) when $\mathcal{R}_0$ is > 1. We use time-dependent control strategy by employing Pontryagin's Maximum Principle to derive conditions for optimal LF control. Furthermore, a partial rank correlation coefficient is adopted for the sensitivity analysis to obtain the model's top rank parameters requiring precise attention for efficacious LF prevention and control.

Keywords: Lassa fever; epidemic; modeling; reproduction number; stability; optimal control

1. Introduction

Lassa fever (LF), also referred to as Lassa haemorrhagic fever, is a severe viral haemorrhagic infection that presents severe public health threats to sub-Saharan African countries [1–10]. The virus that causes LF comes from the family of *arenaviradae* and is known as the Lassa virus (LASV) [4, 10]. LASV was first discovered in Lassa town of Borno state of the northern part of Nigeria in 1969 [11, 12]. LASV infection in humans can occur following effective contact with excreta or secrete of rodent that is contaminated with the faeces or urine of an infected animal reservoir host [13]. Human-to-human transmission is acquired due to exposure to the virus in the blood, tissue, secretions, or excretions of a Lassa virus-infected individual [1, 14]. It is worth noting that casual contact such as skin-to-skin contact without transfer of body fluids does not spread LASV. However, human-to-human transmission is common in health care settings and is also known as nosocomial infection when personal protective equipment (PPE) is not properly used. LASV could also be transmitted through contaminated medical equipment, such as reused needles [14]. Moreover, laboratory or hospitals associated infection of the LASV was reported [2]. LASV is zoonotic (i.e., humans become infected when in contact with an infected animal), and the host of the virus is a multimammate rat (*Mastomys* natalensis), a rodent species that is widespread in West Africa [3, 15]. Ecological factors (such as flooded agricultural activities and rainfall) enhances the transmission of LV by providing favourable condition for rodents population growth [1, 2, 14].

Since its emergence, LASV has caused significant health obstruction in sub-Saharan Africa, particularly the West African region [13]. For instance, the risk areas cover approximately 80, 50 and 40% of Sierra Leone, Liberia, Guinea, and Nigeria, respectively [16]. The yearly prevalence of LF was estimated at 100,000 to 300,000 cases, and approximately 5000 deaths, indicating high morbidity and mortality cases [1, 15]. The epidemics of LF classically last for around seven months. It usually begins in November and ends around May of the subsequent year, with most cases occurring in the first three months of the following year, in addition to sporadic cases reported throughout the year [1, 13].

Approximately, it takes 6–21 days for the symptoms of LF to be apparent. Numerous LF infections (roughly 80%) begin with mild symptoms and, thus, are undetectable. Mild symptoms of LF include moderate fever, weakness and malaise; if untreated, muscle pain, headache, chest pain, and sore throat follows in a few days. In 20% infected individuals, the disease may progress to severe symptoms including haemorrhage (i.e., mouth, nose, and uncontrolled vaginal bleeding or gastrointestinal tract), facial swelling, fluid in the lung cavity, and low blood pressure may be developed [11, 13, 15, 17]. There are currently no approved effective and safe vaccines against LF. However, the antiviral drug ribavirin is an effective treatment for LASV if administered early in the initial phase of the disease [1, 13, 15, 18, 19].

Numerous epidemiological models have been generated and used to gain an understanding of the LF transmission, see for instance [1, 2, 9, 10, 12, 15, 20–23], and the references therein. In particular, an epidemic model of the large-scale LF outbreaks in Nigeria was designed by [1] to examine the interaction between the human (host) and rodent (vector) populations, coupling quarantine, isolation,

and hospitalization. Their study suggests that the initial susceptibility could enlarge for the outbreaks from 2016 to 2019. It also highlighted the similarities in the transmission dynamics driving the three major LF outbreaks in the endemic areas. Onah et al. [15] developed a mathematical model for LF transmission. Their study revealed some basic factors influencing the transmission of LF. They employed the optimal control theory to determine how to reduce the spread of LF with minimum cost. A non-autonomous system of nonlinear ordinary differential equations which revealed the dynamics of LF transmission considering seasonal variation in the birth of *mastomys* was investigated by [12].

Furthermore, the dynamics of LF incorporating the effect of quarantine (as a control strategy), reinfection and environmental transmission were investigated by [9]. Their model was rigorously analyzed and showed the existence of backward bifurcation, which causes difficulty for LF control and suggested the need to manage the rodent vector in the community to control LF transmission effectively. Akhmetzhanov et al. [2] examined the two key seasonal factors fueling the transmission of LF in Nigeria. Their results showed that the seasonal migratory dynamics of rodents play a vital role in regulating the cyclical pattern of LF epidemics. Further simulations of the model revealed that the first nine weeks of the season are considered the high-risk period for LF infection. Moreover, the relationships between disease reproduction number and local rainfall on the dynamics of LF were studied by [21]. Their findings showed significant spatial heterogeneity in the LF outbreaks in different Nigerian regions, indicating clear evidence of the impact of rainfall on LF epidemics in Nigeria.

Thus, in this research, we developed a more sophisticated model for the LF dynamics incorporating environmental transmission as well as differential infectivity. It is worth stating that environmental factors are among the most crucial epidemiological factors affecting LF transmission. We extend previous model proposed in [1] by incorporating various transmission modes, i.e., environmental-to-human transmission and environment-to-rodent transmission route. Furthermore, we also aim to extend previous studies of LF [2, 11, 12, 15, 22] by incorporating environmental factors, hospitalization, symptomatically mild infectious and symptomatically severe infectious stages.

The organization of this work is as follows: In Section 2, an epidemic model is presented and qualitatively analyzed in Section 3. We give numerical results in Section 4 and end the paper with a brief discussion and conclusions in Section 5.

2. Materials and methods

2.1. Epidemic data

Following laboratory confirmation and case definition of LF, we routinely retrieved the weekly epidemiological case data of the LF outbreak for Nigeria reported by the Nigeria Center for Disease Control (NCDC) [24] from January 1 through December 31, 2021. We calculated the weekly cumulative incidence from the data and analyzed the incidence scenario for Nigeria.

2.2. Epidemic model

The model to be designed in this study describes the epidemiological dynamics of LF transmission by utilizing a conventional SEIR-typed model to analyze the transmission dynamics and control strategies of the LF outbreak in Nigeria, taking into account mild and severe cases as well as environmental transmission. Our model distinguishes the different stages of disease progression from

mild to severe symptoms [13]. A proportion of initially mild LF patients remaining at home or in an isolation unit may further generate severe symptoms and be forced to a restricted hospital for proper isolation and better treatment. Many modelling investigations revealed the effect of isolation on the LF infection (where people in this stage can still get LF infection), which greatly impacts the transmission and control of LF; for instance, [25, 26].

We divided the total human population at time t, represented by $N_h(t)$, into sub-populations of susceptible, $S_h(t)$, exposed, $E(t)$, symptomatically mild infectious individuals, $I_m(t)$, symptomatically severe infectious individuals, $I_s(t)$, hospitalized, $H(t)$ and recovered, $R_h(t)$, individuals, so that

$$N_h(t) = S_h(t) + E(t) + I_m(t) + I_s(t) + H(t) + R_h(t).$$

The total rodent (reservoir) population at time t, denoted by $N_r(t)$, is divided into two sub-compartments of susceptible and infectious rodents. Hence, we have

$$N_r(t) = S_r(t) + I_r(t).$$

Also, let V represent the Concentration of the LASV present in the environment, such that both humans and rodents can get infected with LF when in contact with contaminated environment. The infection of LF is largely driven by the prevalence of the disease, reservoir population, human behaviour, and seasonality [1, 2, 21].

We depicted the LF model in Figure 1; the state variables and model parameters (Table 1) fulfil the successive systems of non-linear ordinary differential equations given by,

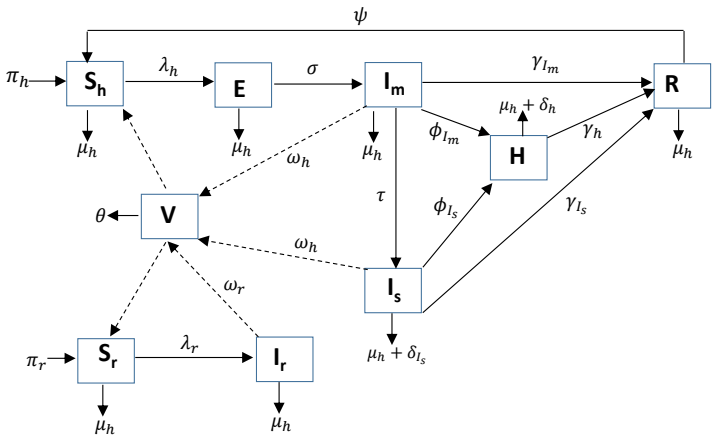

Figure 1. Diagrammatical representation of system (1). Solid arrows designate transitions and expressions next to arrows show the *per ca-pita* flow rate between compartments.

$$
\begin{aligned}
\frac{\mathrm{d}S_h}{\mathrm{d}t} &= \pi_h + \psi R - \lambda_h S_h - \mu_h S_h,\\
\frac{\mathrm{d}E}{\mathrm{d}t} &= \lambda_h S_h - (\sigma + \mu_h)E,\\
\frac{\mathrm{d}I_m}{\mathrm{d}t} &= \sigma E - (\tau + \phi_{I_m} + \gamma_{I_m} + \mu_h)I_m,\\
\frac{\mathrm{d}I_s}{\mathrm{d}t} &= \tau I_m - (\phi_{I_s} + \gamma_{I_s} + \delta_{I_s} + \mu_h)I_s,\\
\frac{\mathrm{d}H}{\mathrm{d}t} &= \phi_{I_m} I_m + \phi_{I_s} I_s - (\gamma_h + \delta_h + \mu_h)H,\\
\frac{\mathrm{d}R}{\mathrm{d}t} &= \gamma_{I_m} I_m + \gamma_{I_s} I_s + \gamma_h H - (\psi + \mu_h)R,\\
\frac{\mathrm{d}V}{\mathrm{d}t} &= \omega_h(I_m + I_s) + \omega_r I_r - \theta V,\\
\frac{\mathrm{d}S_r}{\mathrm{d}t} &= \pi_r - \lambda_r S_r - \mu_r S_r,\\
\frac{\mathrm{d}I_r}{\mathrm{d}t} &= \lambda_r S_r - \mu_r I_r.
\end{aligned}
\tag{1}
$$

Here, the forces of infection for humans and rodents from the model (1) are respectively given by

$$
\lambda_h = \frac{\beta_{I_m} I_m + \beta_{I_s} I_s}{N_h} + \beta_{vh}\frac{V}{k+V} \quad \text{and} \quad \lambda_r = \frac{\beta_r I_r}{N_r} + \beta_{vr}\frac{V}{k+V}. \tag{2}
$$

where, $\frac{\beta_{I_m} I_m + \beta_{I_s} I_s}{N_h}$, $\beta_{vh}\frac{V}{k+V}$, $\frac{\beta_r I_r}{N_r}$, and $\beta_{vr}\frac{V}{k+V}$ represent human-to-human transmission, environment-to-human transmission, rodent-to-rodent transmission, and environment-to-rodent transmission.

2.2.1. The model's elementary characteristics

Since model (1) investigates the dynamics of LF in human and rodent populations, all its state variables and parameters are considered positive. To examine the elementary qualitative features of model (1), we, first of all, consider the rate of change of the total humans $N_h'(t)$ and rodents $N_r'(t)$ populations, which are respectively evaluated as

$$
\frac{dN_h}{dt} = \pi_h - \mu_h N_h - \delta_{I_s} I_2 - \delta_h H \leqslant \pi_h - \mu_h N_h, \tag{3}
$$

and

$$
\frac{dN_r}{dt} = \pi_r - \mu_r N_r, \tag{4}
$$

Furthermore, considering the region,

$$
\Omega = \left\{(S_h, E, I_m, I_s, H, R, V, S_r, I_r) \in \mathbb{R}_+^9 : N_h \leqslant \frac{\pi_h}{\mu_h}, N_r \leqslant \frac{\pi_r}{\mu_r}\right\}.
$$

So that simplifying N_h and N_r given in Eqs (3)–(4) ensure that all solutions of the system that begins in the region Ω will stay in Ω for all non-negative time t (i.e., $t \geqslant 0$). Hitherto, the region Ω is positively-invariant, and it is enough to examine solutions restricted to Ω. Hence, according to previous works [27, 28], the results for usual existence, uniqueness and continuation will be satisfied for model (1).

Table 1. Epidemiological description of the state variables and parameters of model (1)

Variable	Description
N_h	Total humans population
S_h	Susceptible individuals
E	Exposed individuals
I_m	Symptomatically mild infectious individuals
I_s	Symptomatically severe infectious individuals
H	Hospitalized individuals
R	Recovered individuals
V	Concentration of LASV in contaminated environment
N_r	Total rodent population
S_r	Susceptible rodents
I_r	Infectious rodents
Parameter	
$\beta_i (i = I_m, I_s, vh, r, vr)$	Transmission rates
σ	Progression rate
τ	Rate LF progression from I_m to I_s
$\gamma_j (j = I_m, I_s, h)$	Recovery rates period
$\phi_{I_m}(\phi_{I_s})$	Rate of hospitalization from I_m (I_s)
ψ	Rate of relapse from R to S_h
$\delta_{I_s}(\delta_h)$	LF induced death rates
$\omega_h(\omega_r)$	Rate at which the virus is released to the environment
k	Concentration of LASV pathogens in the contaminated environment
θ	Maximum growth rate of the rodents
π_h	Recruitment rate of humans
π_r	Decay rate of LASV pathogens present in the environment
$\mu_h(\mu_r)$	Natural death rate of humans (rodents)

3. Analytical results

3.1. Disease-free equilibrium

Disease-free equilibrium (DFE) of model (1) is obtained by setting all the equations of the right-hand side of model (1) to zero, that is $\frac{dS_h}{dt} = \frac{dE}{dt} = \frac{dI_m}{dt} = \frac{dI_s}{dt} = \frac{dH}{dt} = \frac{dV}{dt} = \frac{dR}{dt} = \frac{dS_r}{dt} = \frac{dI_r}{dt} = 0$. This yields $S_h^0 = \frac{\pi_h}{\mu_h}$, $E^0 = I_m^0 = I_s^0 = H^0 = V^0 = R^0 = 0$, $S_r^0 = \frac{\pi_r}{\mu_r}$, and $I_r^0 = 0$. The DFE point for the proposed model is given by

$$\Gamma^0 = \{S_h^0, E^0, I_m^0, I_s^0, H^0, R^0, V^0, S_r^0, I_r^0\} = \{\frac{\pi_h}{\mu_h}, 0, 0, 0, 0, 0, 0, \frac{\pi_r}{\mu_r}, 0\}.$$

3.2. Basic reproduction number

Here, we computed a basic reproduction number ($\mathcal{R}_0$) of the basic model (1) by adopting the next-generation matrix (NGM) technique as demonstrated in [29]. $\mathcal{R}_0$ represents the number of secondary cases that a typical primary case would cause during the infectious period in a wholly susceptible

population [1, 29–32]. We obtained the linear stability of Γ^0 by implanting similar technique of the NGM on the proposed model (1), with matrices F, which represent the new infection terms, and V, which denote the other transfer terms and are given respectively by

$$\mathcal{F} = \begin{bmatrix} \lambda_h S_h \\ 0 \\ 0 \\ 0 \\ 0 \\ \lambda_r S_r \end{bmatrix} \quad \text{and} \quad \mathcal{V} = \begin{bmatrix} Z_1 E \\ -\sigma E + Z_2 I_m \\ -\tau I_m + Z_3 I_s \\ -\phi_{I_m} I_m - \phi_{I_s} I_s + Z_4 H \\ -\omega I_m - \omega_h I_s - \omega_r I_r + \theta V \\ \mu_r I_r \end{bmatrix},$$

where $Z_1 = \sigma + \mu_h$, $Z_2 = \tau + \phi_{I_m} + \gamma_{I_m} + \mu_h$, $Z_3 = \phi_{I_s} + \gamma_{I_s} + \delta_{I_s} + \mu_h$, $Z_4 = \gamma_h + \delta_h + \mu_h$, and $Z_5 = \psi + \mu_h$. Hence, the LF infection and transition matrices are defined respectively by

$$F = \begin{bmatrix} 0 & C_1 & C_2 & 0 & C_3 & 0 \\ 0 & 0 & 0 & 0 & 0 & 0 \\ 0 & 0 & 0 & 0 & 0 & 0 \\ 0 & 0 & 0 & 0 & 0 & 0 \\ 0 & 0 & 0 & 0 & 0 & 0 \\ 0 & 0 & 0 & 0 & C_4 & C_5 \end{bmatrix} \quad \text{and} \quad V = \begin{bmatrix} Z_1 & 0 & 0 & 0 & 0 & 0 \\ -\sigma & Z_2 & 0 & 0 & 0 & 0 \\ 0 & -\tau & Z_3 & 0 & 0 & 0 \\ 0 & -\phi_m & -\phi_s & Z_4 & 0 & 0 \\ 0 & -\omega_h & -\omega_h & 0 & \theta & -\omega_r \\ 0 & 0 & 0 & 0 & 0 & \mu_r \end{bmatrix}.$$

Direct calculation yields

$$V^{-1} = \begin{bmatrix} {Z_1}^{-1} & 0 & 0 & 0 & 0 & 0 \\ \frac{\sigma_1}{Z_1 Z_2} & {Z_2}^{-1} & 0 & 0 & 0 & 0 \\ \frac{\tau\sigma}{Z_3 Z_1 Z_2} & \frac{\tau}{Z_2 Z_3} & {Z_3}^{-1} & 0 & 0 & 0 \\ \frac{\sigma(\tau\phi_s + Z_3\phi_m)}{Z_3 Z_1 Z_2 Z_4} & \frac{\tau\phi_s + Z_3\phi_m}{Z_2 Z_3 Z_4} & \frac{\phi_s}{Z_3 Z_4} & {Z_4}^{-1} & 0 & 0 \\ \frac{\omega_h\sigma(\tau+Z_3)}{Z_3 Z_1 Z_2\theta} & \frac{\omega_h(\tau+Z_3)}{Z_2 Z_3\theta} & \frac{\omega_h}{Z_3\theta} & 0 & \theta^{-1} & \frac{\omega_r}{\mu_r\theta} \\ 0 & 0 & 0 & 0 & 0 & {\mu_r}^{-1} \end{bmatrix}.$$

and

$$F \cdot V^{-1} = \begin{bmatrix} \frac{C_1\sigma}{Z_1 Z_2} + \frac{\tau C_2\sigma}{Z_3 Z_1 Z_2} + \frac{C_3\omega_h\sigma(\tau+Z_3)}{Z_3 Z_1 Z_2\theta} & \frac{C_1}{Z_2} + \frac{\tau C_2}{Z_2 Z_3} + \frac{C_3\omega_h(\tau+Z_3)}{Z_2 Z_3\theta} & \frac{C_2}{Z_3} + \frac{C_3\omega_h}{Z_3\theta} & 0 & \frac{C_3}{\theta} & \frac{C_3\omega_r}{\mu_r\theta} \\ 0 & 0 & 0 & 0 & 0 & 0 \\ 0 & 0 & 0 & 0 & 0 & 0 \\ 0 & 0 & 0 & 0 & 0 & 0 \\ 0 & 0 & 0 & 0 & 0 & 0 \\ \frac{C_4\omega_h\sigma(\tau+Z_3)}{Z_3 Z_1 Z_2\theta} & \frac{C_4\omega_h(\tau+Z_3)}{Z_2 Z_3\theta} & \frac{C_4\omega_h}{Z_3\theta} & 0 & \frac{C_4}{\theta} & \frac{C_4\omega_r}{\mu_r\theta} + \frac{C_5}{\mu_r} \end{bmatrix}.$$

Therefore, the $\mathcal{R}_0$ is now given by

$$\mathcal{R}_0 = \rho(FV^{-1}) = \mathcal{R}_1 + \mathcal{R}_2 + \mathcal{R}_3, \tag{2}$$

where

$$\mathcal{R}_1 = \left(Z_2\left(C_5\theta + C_4\omega_r\right)Z_1 + \mu_r\sigma\left(\theta C_1 + C_3\omega_h\right)\right)Z_3 + \tau\mu_r\left(C_2\theta + C_3\omega_h\right)\sigma,$$

$$\mathcal{R}_2 = \sqrt{\mathcal{R}_{2a} + \mathcal{R}_{2b} + \mathcal{R}_{2c}}, \quad \text{and}$$

$$\mathcal{R}_3 = \frac{1}{2 * \mu_r\theta Z_3Z_2Z_1},$$

with ρ characterising the spectral radius of the NGM, $C_1 = \frac{\beta_m\mu_h}{\pi_h}$, $C_2 = \frac{\beta_s\mu_h}{\pi_h}$, $C_3 = \frac{\beta_{vh}}{k}$, $C_4 = \frac{\beta_{vr}}{k}$, $C_5 = \frac{\beta_r\mu_r}{\pi_r}$, $R_{2a} = \left(-Z_3Z_1Z_2C_5 + \mu_r\sigma\left(\tau C_2 + C_1Z_3\right)\right)^2\theta^2$,
$R_{2b} = 2\left(\mu_r\sigma C_3\left(\tau + Z_3\right)\omega_h - C_4Z_1Z_2Z_3\omega_r\right)\left(-Z_3Z_1Z_2C_5 + \mu_r\sigma\left(\tau C_2 + C_1Z_3\right)\right)\theta$, and
$R_{2c} = \left(\mu_r\sigma C_3\left(\tau + Z_3\right)\omega_h + C_4Z_1Z_2Z_3\omega_r\right)^2$.

Following [29], and reference to the local stability of the DFE of model (1), we assert the following result.

Theorem 3.1. *The disease-free equilibrium of model* (1) *is locally-asymptotically stable whenever* $\mathcal{R}_0 < 1$ *and unstable if* $\mathcal{R}_0 > 1$.

3.3. Endemic equilibrium

When the LF raids community, it implies that at least one of the infectious classes will be non-empty. Thus, by setting the vector field of the system (1) to zero, we get an endemic equilibrium (EE) state following some algebraic calculation. Thus, the equilibrium point

$$\Gamma^* = \{S_h^*, E^*, I_m^*, I_s^*, H^*, R^*, V^*, S_r^*, I_r^*\}.$$

In terms of E^*, λ_h^* and λ_r^*, the EE points are given by the following equations

$$\begin{aligned}
S_h^* &= \frac{\left(\left(E^*\Psi\sigma\gamma_m + \pi_hz_2z_5\right)z_4 + E^*\phi_m\gamma_h\Psi\sigma\right)z_3 + E^*\Psi\tau\sigma\left(\gamma_h\phi_s + \gamma_sz_4\right)}{z_3z_2z_4z_5\left(\lambda_h^* + \mu_h\right)}\\
I_m^* &= \frac{\sigma E^*}{z_2}\\
I_s^* &= \frac{\sigma\tau E^*}{z_2z_3}\\
H^* &= \left(\phi_{I_m} + \phi_{I_s}\frac{\tau}{Z_3}\right)\frac{\sigma E^*}{Z_2Z_4}\\
R^* &= \frac{\sigma E^*\left(\tau\gamma_h\phi_s + \tau\gamma_sz_4 + \gamma_h\phi_mz_3 + \gamma_mz_3z_4\right)}{z_3z_2z_4z_5}\\
V^* &= \frac{E^*\sigma\omega_h\left(\tau + z_3\right)\mu_r{}^2 + E^*\lambda_r\sigma\omega_h\left(\tau + z_3\right)\mu_r + \omega_r\pi_r\lambda_r^*z_2z_3}{z_2z_3\mu_r\left(\lambda_r^* + \mu_r\right)\theta}\\
S_r^* &= \frac{\pi_r}{\lambda_r^* + \mu_r}, \quad \text{and}\\
I_r^* &= \frac{\pi_r\lambda_r^*}{\mu_r\left(\lambda_r^* + \mu_r\right)}.
\end{aligned} \tag{8}$$

Where

$$\lambda_h^* = \frac{\beta_{I_m} I_m^* + \beta_{I_s} I_s^*}{N_h^*} + \beta_{vh} \frac{V^*}{k + V^*} \quad \text{and} \quad \lambda_r^* = \frac{\beta_r I_r^*}{N_r^*} + \beta_{vr} \frac{V^*}{k + V^*}.$$

Epidemiologically, the existence of EE indicates that at least one of the model's infected classes is non-empty, which means that the LF circulates and persists in a community.

3.4. Stability analysis of the endemic equilibrium

In this sub-section, we analysed the model's solutions in the interior of the feasible region, which converge to the unique EE, given by Γ^*, whenever $\mathcal{R}_0 > 1$. Thus, at Γ^*, the LF will spread and persist in a community. To prove the global stability of the EE, we employed a Lyapunov function technique [33], which is attainable by constructing the Lyapunov function from the model. This method has been used largely in previous studies; for instance, [33–37].

Theorem 3.2. *Under certain conditions (given below), the EE,* Γ^**, is globally-asymptotically stable (GAS) in the region* Ω *whenever* $\mathcal{R}_0 > 1$*. The conditions are* $\left(2 + \frac{\lambda_h}{\lambda_h^*}\right) \leq \frac{S_h^*}{S_h} + \frac{E}{E^*} + \frac{E^* \lambda_h S_h}{E \lambda_h^* S_h^*}$, $\left(2 + \frac{E}{E^*}\right) \leq \frac{I_m^* E}{I_m E^*} + \frac{H}{H^*} + \frac{H^* I_m}{H I_m^*}$, $\left(2 + \frac{I_m}{I_m^*}\right) \leq \frac{I_s^* I_m}{I_s I_m^*} + \frac{H}{H^*} + \frac{H^* I_s}{H I_s^*}$*, and* $\left(\frac{I_m}{I_m^*} - \ln \frac{I_m}{I_m^*} + \frac{I_s}{I_s^*} - \ln \frac{I_s}{I_s^*} + \frac{I_r}{I_r^*} - \ln \frac{I_r}{I_r^*}\right) \leq 3\left(\frac{V}{V^*} - \ln \frac{V}{V^*}\right)$.

The proof of the above Theorem 3.2 is given in Appendix A1.

3.5. Analysis of optimal control

This section employed two control strategies on the proposed LF transmission model, considering $u_1(t)$ as proper sanitation and personal hygiene for the exposed compartment, such as keeping the environment tidy to avert rodents from entering homes as well as using shielding apparatus such as gloves, face masks, goggles and gowns. $u_2(t)$ is considered as the provision of adequate health resources for the mild infectious class, such as providing sufficient antiviral drug ribavirin, which provides effective treatment for LF patients if given early. We aspire to find the optimal controls $(u_1(t), u_2(t))$ required to minimize the number of exposed and mild infectious people together with the cost of controls. So, the control system is given by

$$
\begin{aligned}
\frac{\mathrm{d}S_h}{\mathrm{d}t} &= \pi_h + \psi R - u_1\lambda_h S_h - \mu_h S_h,\\
\frac{\mathrm{d}E}{\mathrm{d}t} &= u_1\lambda_h S_h - (u_2 + \mu_h)E,\\
\frac{\mathrm{d}I_m}{\mathrm{d}t} &= u_2 E - (\tau + \phi_{I_m} + \gamma_{I_m} + \mu_h)I_m,\\
\frac{\mathrm{d}I_s}{\mathrm{d}t} &= \tau I_m - (\phi_{I_s} + \gamma_{I_s} + \delta_{I_s} + \mu_h)I_s,\\
\frac{\mathrm{d}H}{\mathrm{d}t} &= \phi_{I_m} I_m + \phi_{I_s} I_s - (\gamma_h + \delta_h + \mu_h)H,\\
\frac{\mathrm{d}R}{\mathrm{d}t} &= \gamma_{I_m} I_m + \gamma_{I_s} I_s + \gamma_h H - (\psi + \mu_h)R,\\
\frac{\mathrm{d}V}{\mathrm{d}t} &= \omega_h(I_m + I_s) + \omega_r I_r - \theta V,\\
\frac{\mathrm{d}S_r}{\mathrm{d}t} &= \pi_r - \lambda_r S_r - \mu_r S_r,\\
\frac{\mathrm{d}I_r}{\mathrm{d}t} &= \lambda_r S_r - \mu_r I_r.
\end{aligned}
\tag{9}
$$

Where $S_h(0) = S_{h0}, E(0) = E_0, I_m(0) = I_{m0}, I_s(0) = I_{s0}, R(0) = R_0, V(0) = V_0, S_r(0) = L_{r0}, I_r(0) = I_{r0}$. Thus, the objective function required to minimise our problem is defined below

$$
J(u_1, u_2) = \int_0^{t_f} \left(r_1 E + r_2 I_m + \frac{1}{2} w_1 u_1^2 + \frac{1}{2} w_2 u_2^2 \right) \mathrm{d}t, \tag{10}
$$

with, w_1 and w_2 are defined as weight factors. With $u_1, u_2 \in U$ where $U = \{(u_1, u_2) : u_1, u_2,$ are piecewise continuous and $0 \leq u_1, u_2 \leq 1\}$ is the set of permissible controls. It is worth noting that the primary goal is to find the optimal levels of the control functions to converge all the relevant variables that will minimize the objective function.

Thus, we find u_1, u_2, such that $J(u_1^*, u_2^*) = \min_{(u_1,u_2)\in U} J(u_1, u_2)$, is the set of control functions, and the coefficients of the state variables r_1, r_2 and w_1, w_2 are considered to be positive. Since the condition related to the cost is nonlinear, we assume the cost expression to be a quadratic function given by $(\frac{1}{2} w_i u_i^2)$.

3.5.1. Existence of optimal control

Following [38], we established the existence of optimal controls for the LF epidemic. The boundedness of the solution of model 1 ascertained in section two guarantees the existence of the model's solution. For thorough verification, see Theorem 6 of [38].

3.5.2. Hamiltonian and optimality system

Owing to the existence of the optimal controls for LF infection, we employed Pontryagin's Maximum Principle to evaluate the expression of the control functions. To attain this, we first need to define the Hamiltonian $((H_m))$, which is described as follows.

$$
H_m = L + \lambda_1 \frac{dS_h}{dt} + \lambda_2 \frac{dE}{dt} + \lambda_3 \frac{dI_m}{dt} + \lambda_4 \frac{dI_s}{dt} + \lambda_5 \frac{dH}{dt} + \lambda_6 \frac{dR}{dt} + \lambda_7 \frac{dV}{dt} + \lambda_8 \frac{dS_r}{dt} + \lambda_9 \frac{dI_r}{dt} \tag{11}
$$

where L is the Lagrangian acquired from the objective function. Accordingly, the Hamiltonian is now given by

$$\begin{aligned} H_m =& r_1 E + r_2 I_m + \frac{1}{2} w_1 u_1^2 + \frac{1}{2} w_2 u_2^2 \\ &+ \lambda_1 \left(\pi_h + \psi R - u_1 \lambda_h S_h - \mu_h S_h\right) + \lambda_2 \left(u_1 \lambda_h S_h - (u_2 + \mu_h) E\right) \\ &+ \lambda_3 \left(u_2 E - (\tau + \phi_{I_m} + \gamma_{I_m} + \mu_h) I_m\right) + \lambda_4 \left(\tau I_m - (\phi_{I_s} + \gamma_{I_s} + \delta_{I_s} + \mu_h) I_s\right) \\ &+ \lambda_5 \left(\phi_{I_m} I_m + \phi_{I_s} I_s - (\gamma_h + \delta_h + \mu_h) H\right) + \lambda_6 \left(\gamma_{I_m} I_m + \gamma_{I_s} I_s + \gamma_h H - (\psi + \mu_h) R\right) \\ &+ \lambda_7 \left(\omega_h (I_m + I_s) + \omega_r I_r - \theta V\right) + \lambda_8 \left(\pi_r - \lambda_r S_r - \mu_r S_r\right) + \lambda_9 \left(\lambda_r S_r - \mu_r I_r\right) \end{aligned} \tag{12}$$

where $\lambda_1, \lambda_2, \lambda_3, \lambda_4, \lambda_5, \lambda_6, \lambda_7, \lambda_8$ and λ_9 are named the adjoint variables to be expressed. Hence, the following theorem is ascertained.

Theorem 3.3. *Given an optimal control set of u_1 and u_2 together with the corresponding solution, $S_h, E, I_m, I_s, H, R, V, S_r$ and I_r which minimize $J(u_1, u_2)$ over U, then there exist adjoint variables $\lambda_1, \lambda_2, \lambda_3, \lambda_4, \lambda_5, \lambda_6, \lambda_7, \lambda_8$ and λ_9 such that*

$$\begin{aligned} \frac{d\lambda_1}{dt} &= \lambda_1 u_1 \lambda_h + \lambda_1 \mu_h - \lambda_2 u_1 \lambda_h \\ \frac{d\lambda_2}{dt} &= -r_1 + \lambda_2 (u_2 + \mu_h) - \lambda_3 u_2 \\ \frac{d\lambda_3}{dt} &= -r_2 + \lambda_3 \left(\tau + \phi_{I_m} + \gamma_{I_m} + \mu_h\right) - \lambda_4 \tau - \lambda_5 \phi_{I_m} - \lambda_6 \gamma_{I_m} - \lambda_7 \omega_h \\ \frac{d\lambda_4}{dt} &= \lambda_4 \left(\tau + \phi_{I_s} + \gamma_{I_s} + \delta_{I_s} + \mu_h\right) - \lambda_5 \phi_{I_s} - \lambda_6 \gamma_{I_s} - \lambda_7 \omega_h \\ \frac{d\lambda_5}{dt} &= \lambda_5 \left(\gamma_h + \delta_h + \mu_h\right) - \lambda_6 \gamma_h \\ \frac{d\lambda_6}{dt} &= \lambda_6 (\psi + \mu_h) \\ \frac{d\lambda_7}{dt} &= \lambda_6 \theta \\ \frac{d\lambda_8}{dt} &= \lambda_8 (\lambda_r + \mu_r) - \lambda_9 \lambda_r \\ \frac{d\lambda_9}{dt} &= \lambda_7 \omega_r + \lambda_9 \mu_r \end{aligned} \tag{13}$$

with transversality conditions $\lambda_i(t_f) = 0$, $i = 1, ..., 9$. Moreover,

$$\begin{aligned} u_1^* &= \min\left(\max\left(\frac{\lambda_h S_h (\lambda_1 - \lambda_2)}{w_1}, 0\right), 1\right) \\ u_2^* &= \min\left(\max\left(\frac{(\lambda_3 - \lambda_5) E}{w_2}, 0\right), 1\right). \end{aligned} \tag{14}$$

Proof. Considering the existence of the control functions, we employed Pontraygin's Maximum Principle to find the adjoint variables and the expressions of the control functions. Then, we proceed

as follows:

$$\begin{aligned}
\frac{d\lambda_1}{dt} &= -\frac{\partial H_m}{\partial S_h} = \lambda_1 u_1 \lambda_h + \lambda_1 \mu_h - \lambda_2 u_1 \lambda_h \\
\frac{d\lambda_2}{dt} &= -\frac{\partial H_m}{\partial E} = -r_1 + \lambda_2 (u_2 + \mu_h) - \lambda_3 u_2 \\
\frac{d\lambda_3}{dt} &= -\frac{\partial H_m}{\partial I_m} = -r_2 + \lambda_3 (\tau + \phi_{I_m} + \gamma_{I_m} + \mu_h) - \lambda_4 \tau - \lambda_5 \phi_{I_m} - \lambda_6 \gamma_{I_m} - \lambda_7 \omega_h \\
\frac{d\lambda_4}{dt} &= -\frac{\partial H_m}{\partial I_s} = \lambda_4 (\tau + \phi_{I_s} + \gamma_{I_s} + \delta_{I_s} + \mu_h) - \lambda_5 \phi_{I_s} - \lambda_6 \gamma_{I_s} - \lambda_7 \omega_h \\
\frac{d\lambda_5}{dt} &= -\frac{\partial H_m}{\partial H} = \lambda_5 (\gamma_h + \delta_h + \mu_h) - \lambda_6 \gamma_h \\
\frac{d\lambda_6}{dt} &= -\frac{\partial H_m}{\partial R} = \lambda_6 (\psi + \mu_h) \\
\frac{d\lambda_7}{dt} &= -\frac{\partial H_m}{\partial V} = \lambda_6 \theta \\
\frac{d\lambda_8}{dt} &= -\frac{\partial H_m}{\partial S_r} = \lambda_8 (\lambda_r + \mu_r) - \lambda_9 \lambda_r \\
\frac{d\lambda_9}{dt} &= -\frac{\partial H_m}{\partial I_r} = \lambda_7 \omega_r + \lambda_9 \mu_r
\end{aligned} \tag{15}$$

Given the representations of the control functions $\frac{\partial H}{\partial u_i} = 0$ at $u_i = u_i^*$ for $i = 1, 2, ...8$, and following the standard optimality arguments, we have

$$\begin{aligned}
u_1^* &= \min\left(\max\left(\frac{\lambda_h S_h(\lambda_1 - \lambda_2)}{w_1}, 0\right), 1\right) \\
u_2^* &= \min\left(\max\left(\frac{(\lambda_3 - \lambda_5)E}{w_2}, 0\right), 1\right).
\end{aligned} \tag{16}$$

□

Hence, having determined the representations of the control functions u_1^*, u_2^* and the adjoint equations with their transversality conditions. We ensured the existence of the optimal levels needed to minimize the spread of LF infection.

4. Numerical results

4.1. Model prediction

In this part, we employed the previous approach described in [35, 39] to validate/fit the model using the LF surveillance data compiled and published by the NCDC [24]. Pearson's Chi-square and the least square scheme are adopted for the data fitting process using the R statistical software (version 4.1.2). The weekly LF morbidity cases for January through December 2021 (i.e., 52 epidemiological weeks) are used to fit the model to the actual LF scenario. The result shows that the model fitted the LF situation report in Nigeria well with reasonable parameter settings. Figure 2 illustrates the fitting results of LF confirmed cases using the cumulative number of cases for 52 epidemiological weeks.

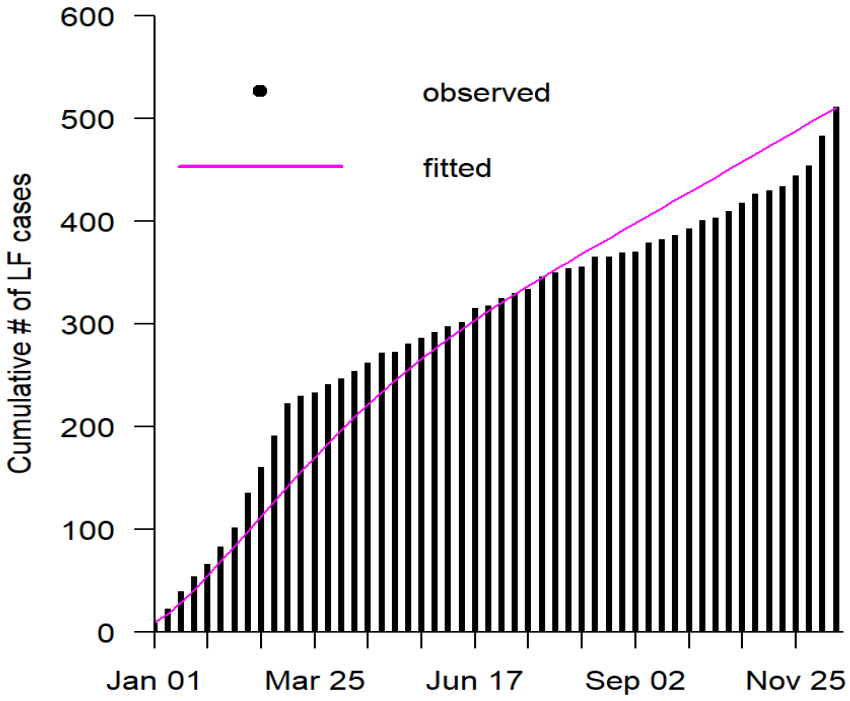

Figure 2. Model fittings result for LF outbreak in Nigeria. Black dots denote actual LF scenario, and the purple curve denote LF model prediction.

Demographic time-series scenarios for LF in Nigeria were obtained from https://www.statista.com/ [42]. And we calculated other related demographic parameters, including π and μ as follows. π is calculated as 9585 per day. Also, since the life expectancy at birth in Nigeria was estimated at 60.87 years in 2021, indicating that $\mu = \frac{1}{60.87\times365}$ per day$= 4.5 \times 10^{-5}$ per day. All other parameters are fixed as in Table 2. It is paramount to note that Edo, Ondo, Ebonyi, and Bauchi established more than 60% of all the LF cases in Nigeria [24]. Figure 2 show the model fitting result for 52 epidemiological weeks (i.e., January to December, 2021). The initial conditions used are given as follows: $S_h(0) = 2.13 \times 10^8$, $E(0) = 164$, $I_m(0) = 20$, $I_s(0) = 9$, $H(0) = 6$, $R(0) = 2$, $V(0) = 10 \times 10^3$, $S_r(0) = S_h(0) \times 10^{-2}$ and $I_r(0) = 76$. Furthermore, from the prediction result, we observed an immediate increase in the number of LF morbidity for the first three months of 2021, which is consistent with prior LF outbreaks in Nigeria [1, 8, 24].

4.2. Numerical simulations

This part presents various numerical findings for the proposed LF model using parameters from Table 2. To simulate the model (1), we utilized the classical Euler numerical technique as described and discussed in [40, 41]. We simulated the presented model using the numerical solver defined above to observe the dynamics of each compartment and several crucial parameters of the model. In particular, in Figure 3(a)–(i), we show the time-series simulation results for the model showing the dynamics features of the state variables using the epidemiological parameter values given in Table 2. Also, in Figure 4(a)–(f), additional simulation results were provided to show the effect of varying the model's key parameters on the overall dynamics of the model.

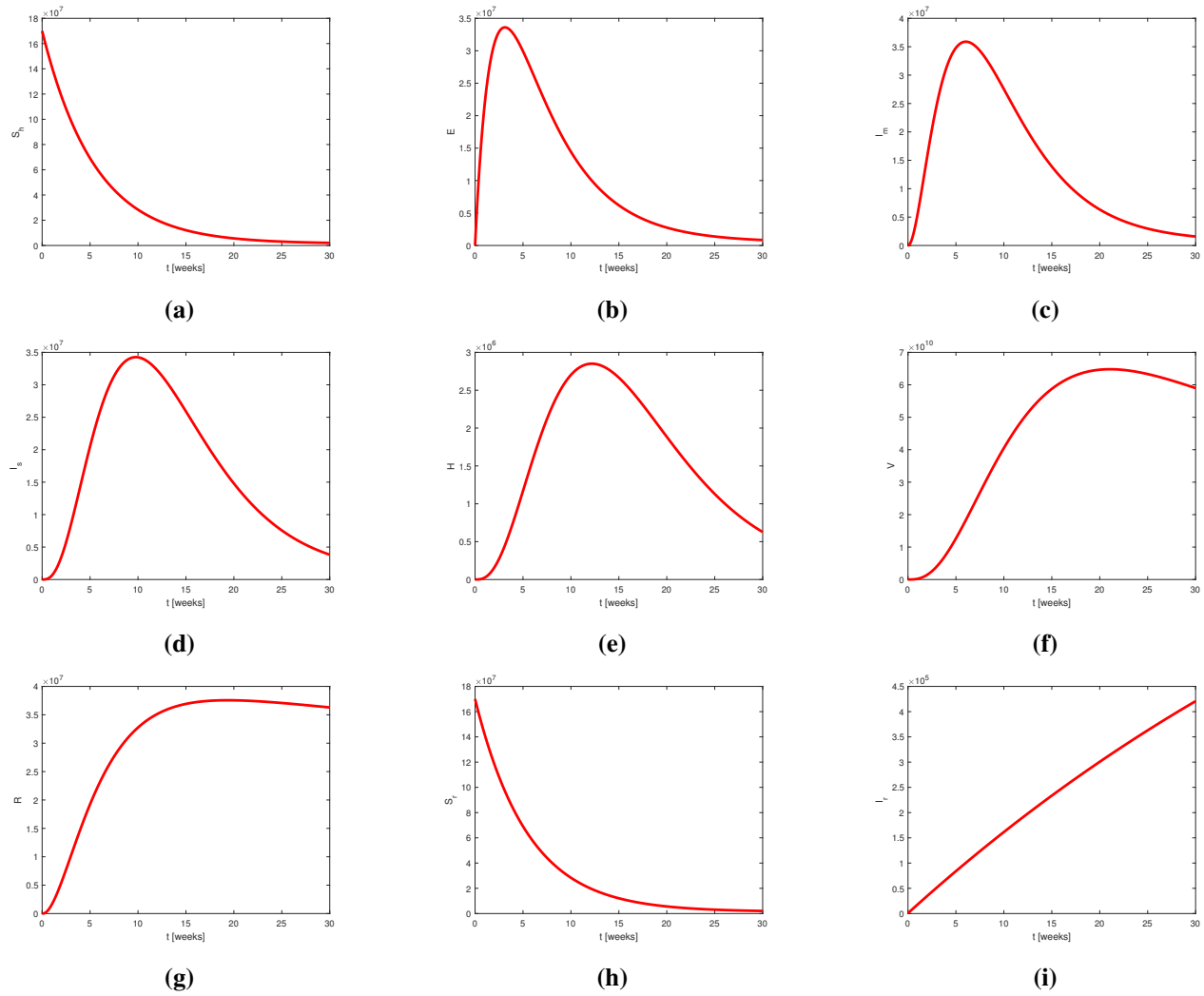

Figure 3. Time-series plots for the state variables of the model showing the dynamical behaviour while using the parameters' values given in Table 2.

Table 2. Summary table for parameters values of model (1)

Parameter	Baseline (Range)	Units	Sources
N_h	2.13×10^8 (1.8×10^8– 2.2×10^8)	Persons	Estimated by [42]
N_r	$0.01 \times N_h$	Rodents	Assumed
μ_h	0.000045 (0.00003–0.00006)	Per day	Estimated by [42]
μ_r	0.002 (0.001–0.006)	Per day	[43]
π_h	2500 (1000–5000)	Persons per day	[1,44]
π_r	0.1 (0– 1)	Rodents per day	Estimated by [45]
k	4000 (2000–10000)	Rodents	[1]
σ	0.52 (0.1–1)	Per day	[1]
τ	0.32 (0.01–0.95)	Per day	Assumed
γ_{I_m}	0.0517 (0–1)	Per day	[1]
γ_{I_s}	0.031 (0–1)	Per day	Estimated by [1]
γ_h	0.035 (0–1)	Per day	Estimated by [1]
ϕ_{I_m}	0.0123 (0.001–0.025)	Per day	[1]
ϕ_{I_s}	0.012 (0.0015–0.025)	Per day	Estimated by [1]
ψ	0.0067 (0.0035–0.03)	Per day	[1]
δ_{I_s}	0.2 (0.1–0.5)	Per day	Estimated by [1]
δ_h	0.19 (0.1–0.5)	Per day	[1]
ω_h	$10^2 - 10^4$	$(TCID)_{50}/ml$	Estimated by [46]
ω_r	$10^3 - 10^5$	$(TCID)_{50}/ml$	[46]
θ	0.033	Per day	[47]
β_{I_m}	0.22 (0.03–0.5)	Per day	[1]
β_{I_s}	0.19 (0.03–0.5)	Per day	Estimated by [1]
β_{vh}	0.12 (0.01–0.7)	Per day	Assumed
β_r	0.142 (0.05–0.4)	Per day	[1]
β_{vr}	0.15 (0.01–0.75)	Per day	Assumed

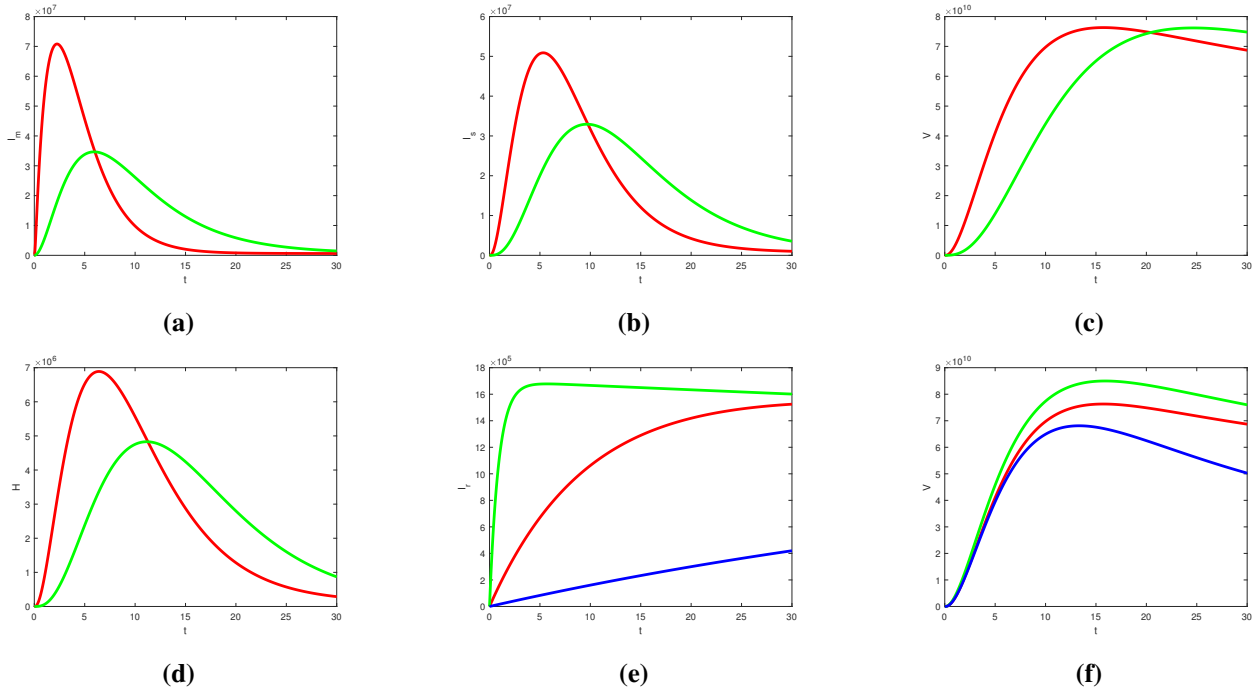

Figure 4. Model simulation results. (a) Increasing and decreasing values for β_r, (b) Increasing and decreasing values for β_{vr}; (c) Increasing and decreasing values for β_{vh}, (d) Increasing and decreasing values for ω_h; (e) Increasing and decreasing values for β_r, (f) Increasing and decreasing values for β_{vr}.

4.3. *Sensitivity analysis*

In this sub-section, we investigated sensitivity analysis to uncover the robust effect and influence of the different model parameters on LF transmission in Nigeria. We adopted the partial rank correlation coefficient (PRCC) to unveil sensitivity analysis of model (1) with consideration of $\mathcal{R}_0$ and infection attack rate as response functions [48]. Our analysis results show that the parameters μ_r, θ and β_r are the most sensitive parameters of the model requiring high observation to mitigate the LF transmission in Nigeria and beyond. The diagrammatic presentation of the PRCC with respect to $\mathcal{R}_0$ and infection attack rate is portrayed in Figure 5. We utilized parameter values given in Table 1 for sensitivity analysis.

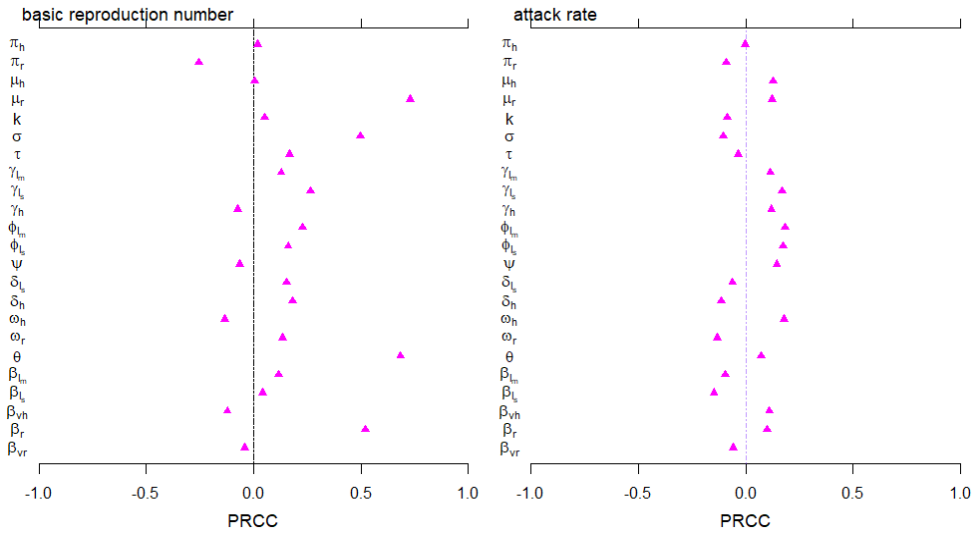

Figure 5. Partial rank correlation coefficient of $\mathcal{R}_0$ and infection attack rate with respect to model parameters. The dots are the estimated correlation, and the bars designate the 95% confidence interval. The parameter values utilised for sensitivity analysis are summarised in Table 2.

5. Discussion and conclusions

Lassa fever is a dominant public health problem in West Africa [4]. It is a distinct viral hemorrhagic fever that affects many sub-Saharan African countries, with Guinea, Liberia, Nigeria, and Sierra Leone as the most endemic countries [6]. LF's severity and mortality cases are alarming, especially in pregnant women; early therapy using ribavirin (and rehydration) helps improve the prevention and control of LF [13, 19]. Moreover, the candidate vaccines currently in development could significantly support the prevention of LF infection and help control neurological complications such as deafness which usually happens to some LF recovered patients [8]. Despite growing public health interest and concern for LF transmission, the knowledge of its ecology, epidemiology, and distribution in West Africa is still limited and needs urgent attention from researchers, public health practitioners, and policymakers.

In this research, we proposed a new deterministic model (see Figure 1) to analyze LF transmission considering mild and severe infection and the role of environmental contribution on the overall LF

infection. The model fitted nicely (see Figure 2) with the LF data for Nigeria and helped investigate the dynamic behaviour of the seasonal LF outbreaks. Our epidemic modelling framework is based on amplifying different infection stages and environmental impacts on the spread of LF. Moreover, our results revealed a better insight into the patterns and driving forces of LF infection in Nigeria. Since LF is a climate and land-use acute disease with poor people as the most vulnerable, there is a need for environmental sanitization, especially in poverty settings, to lower the morbidity and mortality of the disease effectively. LF is presumably driven by ecological factors with the principal host as M. natalensis, which strongly linked LF cases and rainfall [4]. We modelled the dynamics of rodents as constant instead of time-dependent as proposed in [2]. This is due to inadequate data for the rodents population, e.g., population size and disease prevalence among vector populations; thus, we focused our analyses on the human population and environmental factors' contribution to the overall transmission dynamics.

The threshold parameter, $\mathcal{R}_0$, was calculated using the conventional approach of NGM. The $\mathcal{R}_0$ is regarded as one of the most crucial epidemiological quantities used for disease control. Epidemiologically, $\mathcal{R}_0 < 1$ ensures that the LF elimination can be achieved with time even when the control measures are not fully implemented, whereas LF persists in a population whenever $\mathcal{R}_0 > 1$. Furthermore, the proposed model was rigorously analyzed and showed that the DFE is locally and globally-asymptotically stable whenever the $R_0 < 1$ and unstable otherwise. This epidemiologically implies that the LF community transmission can be reduced significantly if $\mathcal{R}_0$ could be reduced to a value less than one. Further analysis also revealed the existence of the EE points of the model, which shows that without adequate control measures, LF transmission will continue and could cause severe outbreaks, leading to increased morbidity and mortality.

Furthermore, we conducted a couple of numerical simulations to study each compartment's dynamics and analyze several crucial parameters of the model. Based on our simulation results, some critical parameters are significantly relevant in increasing or eliminating the LF. Those parameters can also shed light on how to reduce transmission, e.g., by reducing the risks from the vulnerable population, the number of infected persons and stopping the spread of infection from those who have already been infected. To this end, the dynamic feature of the individuals' compartments has been depicted in Figure 3. Figure 4(a) shows the effect of the parameter β_{Im} on the class I_m for some values whereas Figure 4(b) depicts the effect of the parameter β_{Is} on the class I_s. The effect of the parameter β_{vh} on the class V has been depicted in Figure 4(c) whereas Figure 4(d) depicted the effect of ω_h on the class H. The effect of the parameter β_r on the class I_r has been depicted in Figure 4(e) whereas Figure 4(f) depicted the effect of β_{vr} on the class V.

In addition, the PRCC for the sensitivity analysis of model (1) was estimated with $\mathcal{R}_0$ and infection attack rate as response functions (see Figure 5). This revealed that the parameters μ_r (death rate of rodents), θ (growth rate of rodents) and β_r (transmission rate of rodents) are estimated as the model's top-ranked parameters that need emphasis for effective LF control. These parameters are all related to rodents populations, indicating a need to control rodents from the environments for effective LF control.

In conclusion, we qualitatively investigated LF transmission dynamics considering the effect of differential infectivity and environmental factors, which are plausibly the main drivers of Nigeria's LF epidemic. The fitting results of the deterministic model were obtained using the reported LF cases for Nigeria. We observed that the prediction result could be used to assess the transmission patterns

of LF epidemics. Consequently, the effects of environmental factors that drive the LF dynamics were analyzed, considering humans and rodents as hosts and vectors. This study also examined seasonal amplitude that marked the first fifteen epidemiological weeks of the season as the high-risk period for LF outbreaks in Nigeria. Hence, substantial research on LF and the provision of adequate health resources, such as reverse transcriptase polymerase chain reaction assay and antigen detection test kits, as well as antiviral drug ribavirin, are needed to earn sufficient LF prevention and mitigation.

Availability of data and materials

All data used in this research were obtained from public sites.

Acknowledgements

The authors are grateful to the handling editor and anonymous reviewers for the insightful comments.

Conflict of interests

The authors declare that they have no financial or non-financial conflict of interest in this article.

References

1. S. S. Musa, S. Zhao, D. Gao, Q. Lin, G. Chowell, D. He, Mechanistic modelling of the large-scale Lassa fever epidemics in Nigeria from 2016 to 2019, *J. Theoret. Biol.*, **493** (2020), 110209. https://doi.org/10.1016/j.jtbi.2020.110209
2. A. R. Akhmetzhanov, Y. Asai, H. Nishiura, Quantifying the seasonal drivers of transmission for Lassa fever in Nigeria, *Philos. Trans. R. Soc. B*, **374** (2019), 20180268. https://doi.org/10.1098/rstb.2018.0268
3. S. Kenmoe, S. Tchatchouang, J. T. Ebogo-Belobo, A. C. Ka'e, G. Mahamat, R. E. Guiamdjo Simo, et al., Systematic review and meta-analysis of the epidemiology of Lassa virus in humans, rodents and other mammals in sub-Saharan Africa, *PLoS Negl. Trop. Dis.*, **14** (2020), e0008589. https://doi.org/10.1371/journal.pntd.0008589
4. D. W. Redding, R. Gibb, C. C. Dan-Nwafor, E. A. Ilori, R. U. Yashe, S. H. Oladele, et al., Geographical drivers and climate-linked dynamics of Lassa fever in Nigeria, *Nat. Commun.*, **12** (2021), 5759, https://doi.org/10.1038/s41467-021-25910-y
5. R. Gibb, L. M. Moses, D. W. Redding, K. E. Jones, Understanding the cryptic nature of Lassa fever in West Africa, *Pathog. Glob. Health*, **111** (2017), 276–288. https://doi.org/10.1080/20477724.2017.1369643
6. A. N. Happi, C. T. Happi, R. J. Schoepp, Lassa fever diagnostics: past, present, and future, *Curr Opin Virol.*, **37** (2019), 132–138. https://doi.org/10.1016/j.coviro.2019.08.002
7. K. D. Min, J. H wang, M. C. Schneider, Y. So, J. Y. Lee, S. I. Cho, An exploration of the protective effect of rodent species richness on the geographical expansion of Lassa fever in West Africa, *PLoS Negl. Trop. Dis.*, **15** (2021), e0009108. https://doi.org/10.1371/journal.pntd.0009108

8. S. S. Musa, S. Zhao, Z. U. Abdullahi, A. G. Habib, D. He, COVID-19 and Lassa fever in Nigeria: A deadly alliance?, *Int. J. Infect. Dis.*, **117** (2022), 45–47. https://doi.org/10.1016/j.ijid.2022.01.058
9. A. Abdulhamid, N. Hussaini, S. S. Musa, D. He, Mathematical analysis of Lassa fever epidemic with effects of environmental transmission, *Results Phys.*, **35** (2022), 105335. https://doi.org/10.1016/j.rinp.2022.105335
10. A. Thielebein, Y. Ighodalo, Taju A, T. Olokor, R. Omiunu, R. Esumeh, et al., Virus persistence after recovery from acute Lassa fever in Nigeria: a 2-year interim analysis of a prospective longitudinal cohort study, *Lancet Microb.*, **3** (2022), e32–40. https://doi.org/10.1016/S2666-5247(21)00178-6
11. O. J. Peter, A. I. Abioye, F. A. Oguntolu, T. A. Owolabi, M. O. Ajisope, A. G. Zakari, et al., Modelling and optimal control analysis of Lassa fever disease, *Inform. Med. Unlocked*, **20** (2020), 100419. https://doi.org/10.1016/j.imu.2020.100419
12. E. A. Bakare, E. B. Are, O. E. Abolarin, S. A. Osanyinlusi, B. Ngwu, O. N. Ubaka, Mathematical modelling and analysis of transmission dynamics of Lassa fever, *J. Appl. Math.*, **2020** (2020), 6131708, https://doi.org/10.1155/2020/6131708
13. *World Health Organization*, Lassa fever Key Facts, 2017. Available from: https://www.who.int/news-room/fact-sheets/detail/lassa-fever.
14. *Centers for Disease Control and Prevention*, Lassa fever, 2022. Available from: https://www.cdc.gov/vhf/lassa/transmission/index.html.
15. I. S. Onah, O. C. Collins, P. G. Madueme, G. C. Mbah, Dynamical system analysis and optimal control measures of Lassa fever disease model, *Int. J. Math. Sci.*, **2020** (2020). https://doi.org/10.1155/2020/7923125
16. E. Fichet-Calvet, D. J. Rogers, Risk maps of Lassa fever in West Africa, *PLoS Negl. Trop. Dis.*, **3** (2009), e388. https://doi.org/10.1371/journal.pntd.0000388
17. I. S. Abdulraheem, Public health importance of Lassa fever epidemiology, clinical features and current management review of literature, *Afr. J. Clin. Exper. Micro.*, **3** (2002), 33–37. https://doi.org/10.4314/ajcem.v3i1.7349
18. J. Wang, S. Zhao, X. Chen, Z. Huang, M. K. Chong, Z. Guo, et al., The reproductive number of Lassa fever: a systematic review, *J. Trav. Med.*, **28** (2021), taab029. https://doi.org/10.1093/jtm/taab029
19. A. P. Salam, A. Duvignaud, M. Jaspard, D. Malvy, M. Carroll, J. Tarning, et al., Ribavirin for treating Lassa fever: A systematic review of pre-clinical studies and implications for human dosing, *PLoS Negl. Trop. Dis.*, **16** (2022), e0010289. https://doi.org/10.1371/journal.pntd.0010289
20. A. Abdullahi, Modelling of transmission and control of Lassa fever via Caputo fractional-order derivative, *Chaos Solit. Fract.*, **151** (2021), 111271. https://doi.org/10.1016/j.chaos.2021.111271
21. S. Zhao, S. S. Musa, H. Fu, D. He, J. Qin, Large-scale Lassa fever outbreaks in Nigeria: quantifying the association between disease reproduction number and local rainfall, *Epidem. Infect.*, **148** (2020), e4. https://doi.org/10.1017/S0950268819002267

22. A. Abdulhamid, N. Hussaini, Effects of quarantine on transmission dynamics of Lassa fever, *Bayero J. Pure Appl. Sci.*, **11** (2018), 397–407. https://doi.org/10.4314/bajopas.v11i1.64S

23. A. Abidemi, K. M. Owolabi, E. Pindza, Modelling the transmission dynamics of Lassa fever with nonlinear incidence rate and vertical transmission, *Phys. A Stat. Mech. Appl.*, **597** (2022), 127259. https://doi.org/10.1016/j.physa.2022.127259

24. *Nigeria Centre for Disease Control*, Disease Situation Report, 2022. Available from: https://ncdc.gov.ng/diseases/sitreps.

25. A. Denes, A. B. Gumel, Modeling the impact of quarantine during an outbreak of Ebola virus disease, *Infect. Dis. Model.*, **4** (2019), 12–27. https://doi.org/10.1016/j.idm.2019.01.003

26. M. A. Safi, A. B. Gumel, Qualitative study of a quarantine/isolation model with multiple disease stages, *Appl. Math. Comput.*, **218** (2011), 1941–1961. https://doi.org/10.1016/j.amc.2011.07.007

27. K. Okuneye, A. B. Gumel, Analysis of a temperature- and rainfall-dependent model for malaria transmission dynamics, *Math. Biosci.*, **287** (2017), 72–92. http://dx.doi.org/10.1016/j.mbs.2016.03.013

28. N. Hussaini, K. Okuneye, A. B. Gumel, Mathematical analysis of a model for zoonotic visceral leishmaniasis, *Infect. Dis. Model.*, **2** (2017), 455–474. https://doi.org/10.1016/j.idm.2017.12.002

29. P. Van den Driessche, J. Watmough, Reproduction numbers and sub-threshold endemic equilibria for compartmental models of disease transmission, *Math. Biosci.*, **180** (2002), 29–48. https://doi.org/10.1016/s0025-5564(02)00108-6

30. F. B. Agusto, M. I. Teboh-Ewungkem, A. B. Gumel, Mathematical assessment of the effect of traditional beliefs and customs on the transmission dynamics of the 2014 Ebola outbreaks, *BMC Med.*, **13** (2015), 96. https://doi.org/10.1186/s12916-015-0318-3

31. P. Van den Driessche P, Reproduction numbers of infectious disease models, *Infect. Dis. Model.*, **2** (2017), 288–303. https://doi.org/10.1016/j.idm.2017.06.002

32. O. Diekmann, J. A. Heesterbeek, J. A. Metz, On the definition and the computation of the basic reproduction ratio R 0 in models for infectious diseases in heterogeneous populations, *J. Math. Biol.*, **28** (1990),365–382. https://doi.org/10.1007/BF00178324

33. J. P. LaSalle, *The stability of dynamical systems, regional conference series in applied mathematics*, Society for Industrial and Applied Mathematics, 1976.

34. C. Yang, X. Wang, D. Gao, J. Wang, Impact of awareness programs on cholera dynamics: Two modeling approaches, *Bull. Math. Biol.*, **79** (2017), 2109–2131. https://doi.org/10.1007/s11538-017-0322-1

35. S. S. Musa, S. Zhao, N. Hussaini, A. G. Habib, D. He, Mathematical modeling and analysis of meningococcal meningitis transmission dynamics. *Intl. J. Biomath.*, **13** (2020), 2050006. https://doi.org/10.1142/S1793524520500060

36. P. Roop-O, W. Chinviriyasit, S. Chinviriyasit, The effect of incidence function in backward bifurcation for malaria model with temporary immunity, *Math. Biosci.*, **265** (2015), 47–64, https://doi.org/10.1016/j.mbs.2015.04.008

37. S. S. Musa, S. Zhao, H. S. Chan, Z. Jin, D. He, A mathematical model to study the 2014-2015 large-scale dengue epidemics in Kaohsiung and Tainan cities in Taiwan, China, *Math. Biosci. Eng.*, **16** (2019), 3841–3863. https://doi.org/10.3934/mbe.2019190

38. T. S. Farouk, H. Evren, An optimal control approach for the interaction of immune checkpoints, immune system, and BCG in the treatment of superficial bladder cancer, *Eur. Phys. J. Plus*, **133** (2018), 241. https://doi.org/10.1140/EPJP/I2018-12092-0

39. S. S. Musa, N. Hussaini, S. Zhao, D. He, Dynamical analysis of chikungunya and dengue co-infection model, *Dis. Cont. Dyn. Syst. B.*, **25** (2020), 1907. http://doi.org/10.3934/dcdsb.2020009

40. S. S. Musa, I. A. Baba, A. Yusuf, A. S. Tukur, A. I. Aliyu, S. Zhao, et al., Transmission dynamics of SARS-CoV-2: A modeling analysis with high-and-moderate risk populations, *Results Phys.*, **26** (2021), 104290. http://doi.org/10.1016/j.rinp.2021.104290

41. I. A. Baba, A. Yusuf, K. S. Nisar, A. H. Abdel-Atye, T. A. Nofal, Mathematical model to assess the imposition of lockdown during COVID-19 pandemic, *Results Phys.*, **20** (2021), 103716. http://doi.org/10.1016/j.rinp.2020.103716

42. *Statista*, Global No.1 Data Platform, 2022. Available from: https://www.statista.com/.

43. P. Sengupta, The laboratory rat: relating its age with humans, *Int. J. Prev. Med.*, **4** (2013), 624–630.

44. *World Bank*, Data, Population website, 2019. Available from: https://data.worldbank.org/indicator/SP.POP.TOTL?locations=NG.

45. M. M. Jo, B. Gbadamosi, T. O. Benson, O. Adebimpe, A. L. Georgina, Modeling the dynamics of Lassa fever in Nigeria, *J. Egyptian Math. Soc.*, **29** (2021), 1185, https://doi.org/10.1186/s42787-021-00124-9

46. J. B. McCormick, Epidemiology and control of Lassa fever, *Arenaviruses*, (1987), 69–78, https://doi.org/10.1007/978-3-642-71726-0_3

47. E. H. Stephenson, E. W. Larson, J. W. Dominik, Effect of environmental factors on aerosol-induced Lassa virus infection, *J. Med. Virol.*, **14** (1984), 295–303, https://doi.org/10.1002/jmv.1890140402

48. D. Gao, Y. Lou, D. He, T. C. Porco, Y. Kuang, G. Chowell, et al., Prevention and control of Zika as a mosquito-borne and sexually transmitted disease: A mathematical modeling analysis, *Sci. Rep.*, **6** (2016), 28070. https://doi.org/10.1038/srep28070

49. Q. Lin, S. S. Musa, S. Zhao, D. He, Modeling the 2014–2015 Ebola virus disease outbreaks in Sierra Leone, Guinea, and Liberia with effect of high-and low-risk susceptible individuals, *Bull. Math. Biol.*, **82** (2020), 82. https://doi.org/10.1007/s11538-020-00779-y

50. Z. Shuai, P. van den Driessche, Global stability of infectious disease models using Lyapunov functions, *SIAM J. Appl. Math.*, **73** (2013), 1513–1532. https://doi.org/10.1137/120876642

51. G. Q. Sun, J. H. Xie, S. H. Huang, Z. Jin, M. T. Li, L. Liu, Transmission dynamics of cholera: Mathematical modeling and control strategies, *Commun Nonl. Sci. Numer. Simul.*, **45** (2017), 235–244. https://doi.org/10.1016/J.CNSNS.2016.10.007

52. S. S. Musa, S. Zhao, N. Hussaini, S. Usaini, D. He, Dynamics analysis of typhoid fever with public health education programs and final epidemic size relation, *Results Appl. Math.*, **10** (2021), 100153. https://doi.org/10.1016/j.rinam.2021.100153

Appendix

A1. Proof of Theorem 3.2

Proof. To prove Theorem 3.2, we adopted the framework proposed in previous studies [9, 34, 36, 37, 40, 49–52], by constructing a Lyapunov function given below.

$$\begin{aligned} G(t) =& g_1\Big(S_h - S_h^* - S_h^* \ln\frac{S_h}{S_h^*}\Big) + g_2\Big(E - E^* - V^* \ln\frac{E}{E^*}\Big) + g_3\Big(I_m - I_m^* - I_m^* \ln\frac{I_m}{I_m^*}\Big) + \\ & g_4\Big(I_s - I_s^* - I_s^* \ln\frac{I_s}{I_s^*}\Big) + g_5\Big(H - H^* - H^* \ln\frac{H}{H^*}\Big) + g_6\Big(V - V^* - V^* \ln\frac{V}{V^*}\Big) + \\ & g_7\Big(S_r - S_r^* - S_r^* \ln\frac{S_r}{S_r^*}\Big) + g_8\Big(I_r - I_r^* - I_r^* \ln\frac{I_r}{I_r^*}\Big) + . \end{aligned} \tag{A1}$$

Then the derivative of the above Lyapunov function with respect to time (t) is given by

$$\begin{aligned} \dot{G}(t) =& g_1\Big(1 - \frac{S_h^*}{S_h}\Big)\dot{S}_h + g_2\Big(1 - \frac{E^*}{E}\Big)\dot{E} + g_3\Big(1 - \frac{I_m^*}{I_m}\Big)\dot{I}_m + g_4\Big(1 - \frac{I_s^*}{I_s}\Big)\dot{I}_s + g_5\Big(1 - \frac{H^*}{H}\Big)\dot{H} + \\ & g_6\Big(1 - \frac{V^*}{V}\Big)\dot{V} + g_7\Big(1 - \frac{S_r^*}{S_r}\Big)\dot{S}_r + g_8\Big(1 - \frac{I_r^*}{I_r}\Big)\dot{I}_r. \end{aligned} \tag{A2}$$

Simplifying each of the above term (A2) and rearranging, we get

$$g_1\Big(1 - \frac{S_h^*}{S_h}\Big)\dot{S}_h = \ \leq g_1\lambda_h^* S_h^*\Big(1 - \frac{\lambda_h S_h}{\lambda_h^* S_h^*} - \frac{S_h^*}{S_h} + \frac{\lambda_h}{\lambda_h^*}\Big), \tag{A3}$$

$$g_2\Big(1 - \frac{E^*}{E}\Big)\dot{E} = g_2\lambda_h^* S_h^*\Big(\frac{\lambda_h S_h}{\lambda_h^* S_h^*} - \frac{E}{E^*} - \frac{E^*\lambda_h S_h}{E\lambda_h^* S_h^*} + 1\Big), \tag{A4}$$

$$g_3\Big(1 - \frac{I_m^*}{I_m}\Big)\dot{I}_m = g_3\sigma E^*\Big(\frac{E}{E^*} - \frac{I_m}{I_m^*} - \frac{I_m^* E}{I_m E^*} + 1\Big), \tag{A5}$$

$$g_4\Big(1 - \frac{I_s^*}{I_s}\Big)\dot{I}_s = g_4\tau I_m^*\Big(\frac{I_m}{I_m^*} - \frac{I_s}{I_s^*} - \frac{I_s^* I_m}{I_s I_m^*} + 1\Big), \tag{A6}$$

$$g_5\Big(1 - \frac{H^*}{H}\Big)\dot{H} = g_5\phi_{I_m} I_m^*\Big(\frac{I_m}{I_m^*} - \frac{H}{H^*} - \frac{H^* I_m}{H I_m^*} + 1\Big) + g_5\phi_{I_s} I_s^*\Big(\frac{I_s}{I_s^*} - \frac{H}{H^*} - \frac{H^* I_s}{H I_s^*} + 1\Big), \tag{A7}$$

$$\begin{aligned} g_6\Big(1 - \frac{V^*}{V}\Big)\dot{V} =& g_6\omega_h I_m^*\Big(\frac{I_m}{I_m^*} - \frac{V}{V^*} - \frac{V^* I_m}{V I_m^*} + 1\Big) + g_6\omega_h I_s^*\Big(\frac{I_s}{I_s^*} - \frac{V}{V^*} - \frac{V^* I_s}{V I_s^*} + 1\Big) + \\ & g_6\omega_r I_r^*\Big(\frac{I_r}{I_r^*} - \frac{V}{V^*} - \frac{V^* I_r}{V I_r^*} + 1\Big), \end{aligned} \tag{A8}$$

$$g_7\Big(1 - \frac{S_r^*}{S_r}\Big)\dot{S}_r = \ \leq g_7\lambda_r^* S_r^*\Big(1 - \frac{\lambda_r S_r}{\lambda_r^* S_r^*} - \frac{S_r^*}{S_r} + \frac{\lambda_r}{\lambda_r^*}\Big), \tag{A9}$$

$$g_8\Big(1 - \frac{I_r^*}{I_r}\Big)\dot{I}_r = g_8\lambda_r^* S_r^*\Big(\frac{\lambda_r S_r}{\lambda_r^* S_r^*} - \frac{I_r}{I_r^*} - \frac{I_r^*\lambda_r S_r}{I_r\lambda_r^* S_r^*} + 1\Big). \tag{A10}$$

Suppose the function $\Upsilon(\Xi) = 1 - \Xi + \ln\Xi$, then, if $\Xi > 0$ it leads to $\Upsilon(\Xi) \leq 0$. Also, if $\Xi = 1$, $\Upsilon(\Xi) = 0$, thus, $\Xi - 1 \geq \ln(\Xi)$ for any $\Xi > 0$. Let the coefficients of the Lyapunov functions (A1) be given by

$g_1 = g_2 = g_5 = g_6 = g_7 = g_8 = 1$, $g_3 = \frac{\phi_{I_m} I_m^*}{\sigma E^*}$, and $g_4 = \frac{\phi_{I_s} I_s^*}{\tau I_m^*}$. Now, we substitute the above coefficients and Eqs (A3)–(A10) into Eq (A2), we get

$$\begin{aligned}
\dot{G}(t) \leq & \lambda_h^* S_h^* \left(2 - \frac{S_h^*}{S_h} - \frac{E}{E^*} - \frac{E^* \lambda_h S_h}{E \lambda_h^* S_h^*} + \frac{\lambda_h}{\lambda_h^*}\right) + \\
& \phi_{I_m} I_m^* \left(\frac{E}{E^*} - \frac{I_m^* E}{I_m E^*} - \frac{H}{H^*} - \frac{H^* I_m}{H I_m^*} + 2\right) + \\
& \phi_{I_s} I_s^* \left(\frac{I_m}{I_m^*} - \frac{I_s^* I_m}{I_s I_m^*} - \frac{H}{H^*} - \frac{H^* I_s}{H I_s^*} + 2\right) + \\
& \omega_h I_m^* \left(\frac{I_m}{I_m^*} - \ln\left(\frac{I_m}{I_m^*}\right) + \ln\left(\frac{V}{V^*}\right) - \frac{V}{V^*}\right) + \\
& \omega_h I_s^* \left(\frac{I_s}{I_s^*} - \ln\left(\frac{I_s}{I_s^*}\right) + \ln\left(\frac{V}{V^*}\right) - \frac{V}{V^*}\right) + \\
& \omega_r I_r^* \left(\frac{I_r}{I_r^*} - \ln\left(\frac{I_r}{I_r^*}\right) + \ln\left(\frac{V}{V^*}\right) - \frac{V}{V^*}\right) + \\
& \lambda_r^* S_r^* \left(2 - \frac{S_r^*}{S_r} - \frac{I_r}{I_r^*} - \frac{I_r^* \lambda_r S_r}{I_r \lambda_r^* S_r^*} + \frac{\lambda_r}{\lambda_r^*}\right).
\end{aligned} \tag{A11}$$

Thus, Eqs (A1)–(A11) ensure that $\frac{dG}{dt} \leq 0$ provided that $\lambda_h^* S_h^* \left(2 - \frac{S_h^*}{S_h} - \frac{E}{E^*} - \frac{E^* \lambda_h S_h}{E \lambda_h^* S_h^*} + \frac{\lambda_h}{\lambda_h^*}\right) \leq 0$, $\left(\frac{E}{E^*} - \frac{I_m^* E}{I_m E^*} - \frac{H}{H^*} - \frac{H^* I_m}{H I_m^*} + 2\right) \leq 0$, $\left(\frac{I_m}{I_m^*} - \frac{I_s^* I_m}{I_s I_m^*} - \frac{H}{H^*} - \frac{H^* I_s}{H I_s^*} + 2\right) \leq 0$, $\left(\frac{I_m}{I_m^*} - \ln\frac{I_m}{I_m^*} + \frac{I_s}{I_s^*} - \ln\frac{I_s}{I_s^*} + \frac{I_r}{I_r^*} - \ln\frac{I_r}{I_r^*}\right) \leq 3\left(\frac{V}{V^*} - \ln\frac{V}{V^*}\right)$. Consequently, the strict inequality $\frac{dG}{dt} = 0$ is satisfied only for $S_h = S_h^*$, $E = E^*$, $I_m = I_m^*$, $I_s = I_s^*$, $H = H^*$, $R = R^*$, $V = V^*$, $S_r = S_r^*$, and $I_r = I_r^*$. Thus, the EE, Γ^{**}, is the only positive invariant set to the system (1) contained entirely in Ω. Thus, following [33] every solutions of Eq (A2) with initial conditions in Ω converge to Γ^*, as $t \to \infty$. Hence, the positive EE (Γ^*) is globally asymptotically stable (GAS).

□

AIMS Press